Molecular docking of pseudopeptidic imidazoles as selective inhibitors against CYP51 enzyme

Acoplamiento molecular de imidazoles psudopeptídicos como inhibidores selectivos contra la enzima CYP51

Yonatan Mederos-Nuñez[1*] http://orcid.org/0000-0003-3163-5810

Armando Ferrer-Serrano[1] http://orcid.org/0000-0002-6849-0232

Raidel Rosales-Rosabal[1] https://orcid.org/0000-0001-9960-141X

Rebeca Joa-Acree[1] https://orcid.org/0009-0008-9122-0020

América García-López[1] http://orcid.org/0000-0003-3773-887X

[1]Department of Chemistry, Natural and Exact Sciences Faculty, Universidad de Oriente, Santiago de Cuba, Cuba

*Corresponding author: email: jmederos@uo.edu.cu

ABSTRACT

P450 family, especially CYP51 protein, is a common target for the design of antifungal and antiprotozoal drugs. Designing new effective drugs against these pathogens is a necessity and a challenge for the scientific community. To this end, they are evaluated by molecular docking of five schemes of aryl-substituted imidazoles and pseudopeptic imidazoles against CYP51 proteins from different pathogens and against the similar human protein to estimate their selectivity. Once these calculations have been carried out, none of the compounds studied appears to be an effective inhibitor against CYP51-*L.infantum*. However, for all the remaining proteins lower normalized coupling scores are obtained, fundamentally for schemes 1 and 3. Given the geometry of the protein-linked complexes formed, schemes 2 and 4 appear to be more selective than schemes 1, 3 and 5. However, the highest estimated selectivity values are obtained for schemes 1 and 3 against CYP51-*C.glabrata* and for scheme 1 against CYP51-*N.fowleri*. In general, the direct relationship between the stability of the protein-ligated complex with the

direct interaction of the ligand with the Fe^{2+} cation of the heme group, which provides stability to the union.

Keywords: molecular docking; CYP51; pseudopeptide imidazoles; selectivity coefficient.

RESUMEN

La familia P450, y en especial la proteína CYP51, es blanco común para el diseño de fármacos antimicóticos y antiprotozoarios. Diseñar nuevos fármacos efectivos contra estos patógenos es una necesidad y un reto para la comunidad científica. Con este objetivo se evalúan mediante acoplamiento molecular de cinco esquemas de imidazoles arilsustituidos e imidazoles pseudopeptídicos contra proteínas CYP51 de distintos patógenos y contra la similar proteína humana para estimar su selectividad. Una vez realizado estos cálculos se arriba a que ninguno de los compuestos estudiados parece ser un inhibidor efectivo contra CYP51-*L.infantum*. Sin embargo, para todas las restantes proteínas se obtienen menores puntuaciones normalizadas del acoplamiento, fundamentalmente para los esquemas 1 y 3. Dada la geometría de los complejos proteína-ligado formados los esquemas 2 y 4 se muestran más selectivos que los esquemas 1, 3 y 5. Sin embargo, los mayores valores de selectividad estimada se obtienen para los esquemas 1 y 3 contra CYP51-*C.glabrata* y para el esquema 1 contra CYP51-*N.fowleri.* De manera general, se constata la relación directa entre la estabilidad del complejo proteína-ligado con la interacción directa del ligando con catión Fe^{2+} del grupo heme, la cual aporta estabilidad a la unión.

Palabras clave: acoplamiento molecular; CYP51, imidazoles pseudopeptídicos; índice de selectividad.

Recibido: 28/4/2023

Aprobado: 20/6/2023

Introduction

Sterol 14-demethylase (CYP51) is the only cytochrome P450 (CYP) required for sterol biosynthesis in different phyla, and is the most widely distributed P450 gene family found in all biological kingdoms: animals, plants, fungi, yeasts, lower eukaryotes, and bacteria.[(1)] The CYP51 family is very special in that its members retain strict functional

conservation in enzymatic activity across all biological kingdoms. With amino acid identity in the kingdoms as low as 25-30 % (about 40 amino acid residues), they all catalyze the first step following cyclization in sterol biosynthesis, where the 14-methyl group is converted to an alcohol, then into an aldehyde. This is then removed as formic acid in the final step, leading to the formation of the initial substrate in steroid hormone biosynthesis.[2]

Some of these substrates form cholesterol (animals), ergosterol (fungi) and a variety of 24 alkylated and olefinated products in plants and protists. Sterols stabilize membranes, determine their fluidity and permeability, and also serve as precursors for biologically active molecules essential for the regulation of growth and development.[2] Furthermore, since humans consume dietary cholesterol which downregulates sterol biosynthesis, this enzyme is an attractive target for antifungal agents in human medicine, veterinary medicine, and for fungicides in agriculture, provided that the selectivity over mammalian CYP51.[3]

In protozoa, the sterol biosynthesis pathway is absent in strict anaerobic organisms, including the human pathogens *Giardia*, *Entamoeba*, *Cryptosporidium*, and *Trichomonas*. However, the sterol biosynthesis pathway is present in free-living amoebae, *Acanthamoeba* and *Naecanthamoeba* belonging to several different *Aecanthamoebae*. Sterols are synthesized from squalene in kinetoplastid protozoa, *Trypanosoma cruzi*, *Trypanosoma brucei*, and *Leishmania* species, the causative agents of Chagas disease, African sleeping sickness, and different forms of leishmaniasis, respectively, which collectively affect hundreds of million people, primarily the poor and underserved, and which have been designated by the WHO as neglected tropical diseases (NTDs).[3]

Most of the currently used clinical antifungal drugs (azoles) are intended to inhibit fungal sterol 14α-demethylase (CYP51). These are based on two precursor compounds: ketoconazole (imidazole) and fluconazole (azole), all of them selected based on their antiparasitic activity in cell experiments.[4] Azole antifungal agents selectively target fungal CYP51 enzymes over the human homolog through the direct coordination of the triazole ring N-4 nitrogen (fluconazole, itraconazole and voriconazole) or the imidazole ring N-3 nitrogen (clotrimazole and ketoconazole) with the heme iron as the sixth axial ligand and the azole drug side chains interact with the CYP51 polypeptide backbone.

Azole antifungals can also coordinate with the heme iron of other cytochrome P450 enzymes, raising the potential for alternate and secondary drug targets.[5]

In recent years, with the widespread use of CYP51-targeting drugs, drug-resistant *Candida*, *Cryptococcus,* and *Aspergillus* have emerged continuously [6] and has become a serious challenge for public health.[7] This makes the search for new inhibitors an area of research for scientists around the world. Currently, development of new CYP51 inhibitors is focuses on new azoles [8], triazines [9], nonazoles [10] and other nitrogenous heterocycles.[11; 12]

However, azole antifungals cause hepatotoxicity by inducing expression of liver cytochrome P450 enzymes (CYP1, CYP2, and CYP3 families), which in turn increases the abundance of reactive oxygen species in liver cells, resulting in lipid peroxidation and DNA damage. In addition, azole antifungals have the potential to inhibit liver P450 enzymes, interfering with phase I metabolism of xenobiotics. In studies in mice, ketoconazole, itraconazole, and propiconazole produced the formation of benign and malignant liver tumors. Additionally, disruption of the endocrine system can lead to reproductive problems, impaired sexual differentiation, growth and development problems, and the formation of hormone-dependent cancers.[13] Therefore, it is vital to consider the selectivity coefficient with respect to human CYP51 in the synthesis of new drugs.

Lead selectivity can also be assessed *in silico* at early stages of drug discovery via molecular docking and comparative modeling of newly designed inhibitors against the structures for human CYP enzymes.[3] Computational techniques such as molecular docking and molecular dynamics have been used to predict this affinity for the pathogenic protein over the human one.[14] That is why in the present investigation an estimate of the inhibition of sterol 14-demethylase (CYP51) of all the pathogenic organisms available in the Protein Data Bank [15] is carried out, as well as its selectivity coefficient with respect to human CYP51 by molecular docking. All this with the objective of evaluating the feasibility of designing aryl-substituted imidazoles and imidazoles functionalized with amino acids (pseudopeptide imidazoles) as possible selective inhibitors of this protein.

Materials and methods

Computational resources

The Molecular modeling was performed using the high-performance computing capabilities of the cluster of the Universidad de Oriente, Cuba (HPC-UO) (https://portal.uo.hpc.cu/website/ (accessed on 6 November 2022)).

Molecular modeling of proteins and ligands for docking

To facilitate understanding, the compounds studied have been divided into five schemes (Figure 1). Schemes 1 and 2 correspond to pseudopeptic imidazoles with phenyl groups in positions 4 and 5, while schemes 3 and 4 present a phenyl group in position 4 and a methyl group in position 5, which from now on will be called asymmetric pseudopeptide imidazoles. For its part, scheme 5 corresponds to tetra- and tri-substituted imidazoles without amino acid residues. To obtain the structures of the pseudopeptic imidazoles and imidazoles, the OpenBabel 3.1.1 program [16] was employed using the molecular mechanics method with the MMFF94 force field (Merck Molecular Force Field).

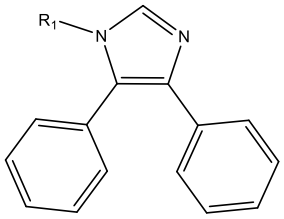

1a R=GLY; **1b** R=ALA; **1c** R=VAL; **1d** R=ARG; **1e** R=GLN; **1f** R=LYS; **1g** R=THR; **1h** R=ASN; **1i** R=TPR; **1j** R=HIS; **1k** R=PHE; **1l** R=GLU; **1m** R=ASP; **1n** R=TYR

cheme 1

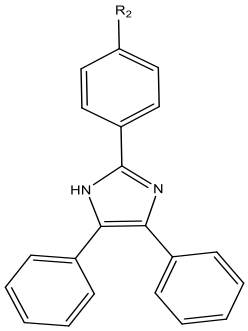

2a R=GLY; **2b** R=ALA; **2c** R=VAL; **2d** R=ARG; **2e** R=GLN; **2f** R=LYS; **2g** R=THR; **2h** R=ASN; **2i** R=TPR; **2j** R=HIS; **2k** R=PHE; **2l** R= TYR; **2m** R=PRO; **2n** R=CYS

Scheme 2

3a R=GLY; **3b** R=ALA; **3c** R=VAL; **3d** R=ARG; **3e** R=GLN; **3f** R=LYS; **3g** R=THR; **3h** R=ASN; **3i** R=TPR; **3j** R=HIS; **3k** R=PHE; **3l** R=GLU; **3m** R=ASP; **3n** R=TYR

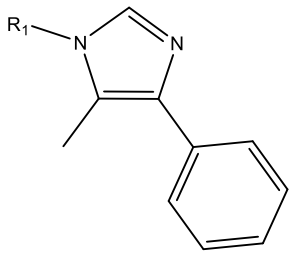

Scheme 3

4a R=GLY; **4b** R=ALA; **4c** R=VAL; **4d** R=ARG; **4e** R=GLN; **4f** R=LYS; **4g** R=THR; **4h** R=ASN; **4i** R=TPR; **4j** R=HIS; **4k** R=PHE; **4l** R= TYR; **4m** R=PRO; **4n** R=CYS

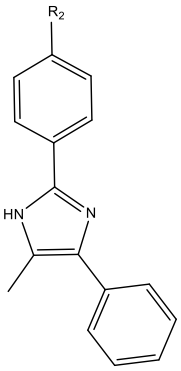

Scheme 4

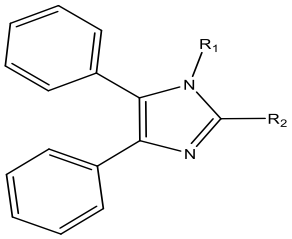

p01	R1= $-C_6H_5$	R2= $-C_6H_5$	**p19**	R1= -H	R2= $-C_6H_5$
p02	R1= $-C_6H_5$	R2= $-C_6H_5-pN(CH_3)_2$	**p20**	R1= -H	R2= $-C_6H_5-pN(CH_3)_2$
p03	R1= $-C_6H_5$	R2= $-C_6H_5$-p(OH)	**p21**	R1= -H	R2= $-C_6H_5$-p(OH)
p04	R1= $-C_6H_5$	R2= $-C_6H_5-p(OCH_3)$	**p22**	R1= -H	R2= $-C_6H_5-p(OCH_3)$

p05	R1= -C_6H_5	R2= -C_6H_5-m(NO_2)		**p23**	R1= -H	R2= -C_6H_5-m(NO_2)	
p06	R1= -C_6H_5	R2= -C_6H_5-p(NO_2)		**p24**	R1= -H	R2= -C_6H_5-p(NO_2)	
p07	R1= -C_6H_5-p(CH_3)	R2= -C_6H_5		**p25**	R1= -C_6H_5-p(SO_3)	R2= -C_6H_5	
p08	R1= -C_6H_5-p(CH_3)	R2= -C_6H_5-p$N(CH_3)_2$		**p26**	R1= -C_6H_5-p(SO_3)	R2= -C_6H_5-p$N(CH_3)_2$	
p09	R1= -C_6H_5-p(CH_3)	R2= -C_6H_5-p(OH)		**p27**	R1= -C_6H_5-p(SO_3)	R2= -C_6H_5-p(OH)	
p10	R1= -C_6H_5-p(CH_3)	R2= -C_6H_5-p(OCH_3)		**p28**	R1= -C_6H_5-p(SO_3)	R2= -C_6H_5-p(OCH_3)	
p11	R1= -C_6H_5-p(CH_3)	R2= -C_6H_5-m(NO_2)		**p29**	R1= -C_6H_5-p(SO_3)	R2= -C_6H_5-m(NO_2)	
p12	R1= -C_6H_5-p(CH_3)	R2= -C_6H_5-p(NO_2)		**p30**	R1= -C_6H_5-p(SO_3)	R2= -C_6H_5-p(NO_2)	
p13	R1= -CH_2-C_6H_5	R2= -C_6H_5		**p31**	R1= -C_6H_5-p(SO_2NH_2)	R2= -C_6H_5	
p14	R1= -CH_2-C_6H_5	R2= -C_6H_5-p$N(CH_3)_2$		**p32**	R1= -C_6H_5-p(SO_2NH_2)	R2= -C_6H_5-p$N(CH_3)_2$	
p15	R1= -CH_2-C_6H_5	R2= -C_6H_5-p(OH)		**p33**	R1= -C_6H_5-p(SO_2NH_2)	R2= -C_6H_5-p(OH)	
p16	R1= -CH_2-C_6H_5	R2= -C_6H_5-p(OCH_3)		**p34**	R1= -C_6H_5-p(SO_2NH_2)	R2= -C_6H_5-p(OCH_3)	
p17	R1= -CH_2-C_6H_5	R2= -C_6H_5-m(NO_2)		**p35**	R1= -C_6H_5-p(SO_2NH_2)	R2= -C_6H_5-m(NO_2)	
p18	R1= -CH_2-C_6H_5	R2= -C_6H_5-p(NO_2)		**p36**	R1= -C_6H_5-p(SO_2NH_2)	R2= -C_6H_5-p(NO_2)	

Scheme 5

Fig .1- Schemes of the compounds studied

For molecular modeling of proteins, their three-dimensional structures were obtained in "pdb" format, from the Protein Data Bank.[15] For refining these structures, generally

obtained by X-ray diffraction, the UCSF Chimera software version 1,10,227 [17] was used. All residues from the crystallization of the macromolecule that do not belong as such to proteins in their natural state and could interfere were identified with their active centers and, therefore, with the interpretation of the results.

The molecular docking study was carried out through the AutoDock-GPU version 15 [18] and AutoDock Tools 1.5.6 programs. The Gasteiger charge calculation method was used and partial charges were added to the ligand atoms prior to docking, via Autodock Tools. The two-dimensional visualization of the hydrophobic and hydrogen bonding interactions of the complexes was carried out using the Ligplot^{+} v.2.2 [19] program and UCSF Chimera version 1.10.227.[17]

The proteins selected for this study correspond to Cytochrome P450, lanosterol 14α demethylase CYP51 and their data are listed in table 1.

Table 1.Proteins used in the study.

PDBID	Organism	Inhibitor	ID Inh.	Resolution (Å)
1X8V	*Mycobacterium tuberculosis*	1,3,5(10)-estratriene-3,16,17-triol	E8L	1,55
3L4D	*Leishmania infantum*	2-(2,4-difluorophenyl)-1,3-di(1H-1,2,4-triazol-1-yl)propan-2-ol	TPF	2,75
4C27	*Trypanosoma cruzi*	nalpha-(2-fluoro-4-{4-[4-(trifluoromethyl)phenyl]piperazin-1-yl}benzoyl)-N-pyridin-4-yl-d-tryptophanamide	26N	1,95
4G3J	*Trypanosoma brucei*	N-[(1R)-1-(2,4-dichlorophenyl)-2-(1H-1,2,4-triazol-1-yl)ethyl]-4-(5-phenyl-1,3,4-oxadiazol-2-yl)benzamide	VNT	1,83
4UYM	*Aspergillus fumigatus*	(2r,3s)-2-(2,4-difluorophenyl)-3-(5-fluoropyrimidin-4-yl)-1-(1h-1,2,4-triazol-1-yl)butan-2-ol (voriconazole)	VOR	2,55
5JLC	*Candida glabrata*	2-[(2r)-butan-2-yl]-4-{4-[4-(4-{[(2r,4s)-2-(2,4-dichlorophenyl)-2-(1h-1,2,4-triazol-1-ylmethyl)-1,3-dioxolan-4-yl]methoxy}cphenyl)piperazin-1-yl]phenyl}-2,4-dihydro-3h-1,2,4-triazol-3-one	1YN	2,40
5TL8	*Naegleria fowleri*	4-(4-(4-(4-(((3R,5R)-5-((1H-1,2,4-triazol-1-yl)methyl)-5-(2,4-difluorophenyl)tetrahydrofuran-3-yl)methoxy)phenyl)piperazin-1-yl)phenyl)-2-((2S,3S)-2-hydroxypentan-3-yl)-2,4-dihydro-3H-1,2,4-triazol-3-one (posaconazole)	X2N	1,71
5TZ1	*Candida albicans*	(R)-2-(2,4-difluorophenyl)-1,1-difluoro-3-(1H-tetrazol-1-yl)-1-(5-(4-(2,2,2-trifluoroethoxy)phenyl)pyridin-2-yl)propan-2-ol	VT1	2,00
6Q2C	*Acanthamoeba castellanii str. Neff*	-	-	1,80
7TEF	*Mycobacterium marinum*	2-[bis-(2-hydroxy-ethyl)-amino]-2-hydroxymethyl-propane-1,3-diol	BTB	1,98
6UEZ	*Homo sapiens*	Lanosterol	LAN	1,98

Selection of molecular docking parameters

AutoDock requires a pre-calculation of the grid maps, which in turn requires a series of related parameters. AutoDock requires pre-calculated grid maps, one for each atom type, present in the ligand being docked as it stores the potential energy arising from the interaction with macromolecule. This grid must surround the region of interest (active site) in the macromolecule. In the present study, the binding site was selected based on the position of the co-crystallized ligand, except for the CYP51-*Acanthamoeba castellanii str. Neff* protein, for which the position of the heme group was taken as a reference, since it is known that it is part of the active site. The selected spacing was 0.375 Å and the grid box size was 60·60·60 points. In addition to this, the location coordinates of the ligand around the region of the active site of the macromolecule are needed, which is shown in table 2.

Table 2. Location of the ligand around the region of the active site of the macromolecules studied.

PDBID	X	Y	Z
4C27	-4,091	13,016	-18,884
4G3J	-10,234	5,761	-6,193
3L4D	30,730	-28,203	-1,418
7TEF	-18,384	9,156	-31,600
6Q2C	0,402	-36,083	5,398
5TZ1	71,526	65,266	5,677
5TL8	3,450	19,302	47,776
5JLC	-42,977	78,373	-21,679
4UYM	135,863	196,666	3,673
1X8V	-34,055	4,754	61,847
6UEZ	-24,476	-37,092	12,137

The Lamarckian Genetic Algorithm (LGA) was used to explore the best conformational space for the ligand, with a minimum of 100 runs for each of the couplings. The calculation was adjusted to a number of energy evaluations of $25 \cdot 10^6$. In analyzing the docking scores, we accounted for the recognized bias due to molecular weight using the equation 1,

$$DSnorm = Edock \cdot 7.2 \cdot \sqrt[5]{MW} \quad (1)$$

where

DSnorm is the normalized docking score, Edock is the MolDock re-rank score,

MW is the molecular weight, and 7.2 is a scaling constant to ensure the average DSnorm values are comparable to those of Edock.[20] The use of this parameter is necessary because the studied ligands present a difference of up to 531.44 $g \cdot mol^{-1}$.

Docking calculations can be validated by calculating root mean square deviation (RMSD),[21] redocking the ligands that were co-crystallized in the receptor structures.[22; 23] This procedure was carried out for all the proteins studied, except in the

case of CYP51-*Acanthamoeba castellanii str. Neff* that does not have co-crystallized inhibitors. It is considered that if the RMSD value of the known conformation is less than 2 Å, the molecular docking has worked successfully.[24]

With the aim of having a criterion that quantifies the selectivity of the compounds studied, a calculable parameter was defined through the results of molecular docking. This parameter was called the selectivity coefficient (SC) and is calculated using equation 2:

$$SC = Ki_p / Ki_h \qquad (2)$$

where

Ki_p is the inhibition constant calculated from normalized docking score for a pathogen CYP51

Ki_h is the inhibition constant calculated from normalized docking score for a human CYP51.

Results and discussion

The molecular docking results for the pseudopeptic imidazoles with the CYP51 enzyme and the ligands co-crystallized with their corresponding enzymes and the RMSD scores are summarized in table 3.

Table 3. Docking scores, normalized for molecular weight (DSnorm, kcal/mol) of pseudopeptic imidazoles with CYP51 molecular targets and RMSD score (Å).

Comp.	1x8v	3l4d	4c27	4g3j	4uym	5jlc	5tl8	5tz1	6q2c	6uez	7tef
1a	-9,34	-9,90	-12,73	-12,31	-10,83	-21,59	-15,66	-13,37	-11,95	-12,21	-6,52
1b	-8,79	-9,94	-12,14	-11,96	-10,90	-20,66	-14,28	-13,40	-11,29	-12,17	-6,10
1c	-8,19	-10,34	-12,37	-10,74	-11,03	-19,20	-13,33	-13,46	-8,50	-12,60	-6,48
1d	-10,96	-9,89	-12,78	-13,01	-12,00	-21,83	-15,49	-14,03	-10,87	-12,32	-7,95
1e	-8.77	-10.76	-12.35	-11.63	-10.89	-19.70	-11.98	-12.74	-9.65	-12.32	-7.82
1f	-8.44	-10,20	-11,91	-12,34	-11,26	-20,79	-13,66	-13,72	-9,98	-12,33	-6,54
1g	-6,79	-9,50	-11,87	-10,74	-10,44	-19,21	-11,59	-12,91	-9,45	-11,62	-6,50
1h	-7,87	-9,38	-11,48	-10,36	-10,15	-19,18	-14,14	-12,19	-8,30	-11,25	-5,61
1i	-7,84	-9,79	-12,03	-12,03	-10,56	-19,62	-14,00	-13,15	-9,45	-11,75	-6,77
1j	-8,68	-11,31	-13,51	-12,39	-11,86	-20,75	-13,73	-14,51	-10,04	-13,99	-7,90
1k	-11,67	-9,62	-12,69	-12,39	-11,46	-21,11	-15,78	-13,54	-10,74	-12,27	-6,46
1l	-11,69	-9,64	-12,81	-12,42	-11,43	-21,08	-15,54	-13,53	-10,65	-12,18	-6,38
1m	-11,64	-9,63	-12,80	-12,39	-11,46	-21,44	-15,59	-13,53	-10,68	-12,30	-6,43
1n	-11,67	-9,63	-12,76	-12,38	-11,43	-21,23	-15,66	-13,54	-10,66	-12,18	-6,39
2a	-7,06	-8,82	-7,39	-7,76	-5,33	-6,52	-7,98	-7,84	-6,84	-3,92	-6,49
2b	-7,27	-8,73	-7,88	-8,04	-5,86	-7,65	-7,77	-8,37	-4,53	-3,91	-6,91
2c	-7,29	-8,84	-7,75	-8,08	-4,90	-7,46	-8,23	-7,18	-3,79	-2,62	-7,33
2d	-8,65	-9,27	-8,15	-9,06	-3,59	-6,08	-9,15	-6,95	-1,15	-3,16	-7,85
2e	-7,74	-8,55	-7,15	-7,80	-4,20	-6,33	-8,65	-6,75	-3,49	-3,05	-7,56
2f	-8,44	-8,51	-7,22	-7,60	-3,56	-4,68	-8,42	-6,29	-2,58	-2,13	-7,19
2g	-7,31	-8,41	-6,97	-7,28	-3,98	-6,98	-7,97	-7,50	-2,80	-2,46	-7,46
2h	-7,47	-8,41	-7,19	-7,57	-4,35	-6,70	-7,90	-6,76	-3,87	-2,77	-8,03
2i	-6,23	-10,24	-8,35	-9,30	-2,37	-6,38	-9,66	-8,31	-0,50	-3,04	-7,66
2j	-7,88	-8,67	-7,39	-8,07	-4,19	-4,83	-8,04	-7,06	-1,75	-3,37	-7,32
2k	-8,45	-9,94	-8,37	-8,45	-3,35	-5,87	-8,95	-7,94	-0,88	-3,44	-7,77
2l	-8,28	-9,21	-7,55	-8,16	-3,32	-5,28	-9,14	-7,68	-0,71	-1,29	-8,39
2m	-6,72	-9,25	-7,47	-7,98	-7,38	-6,56	-8,72	-7,49	-5,53	-6,03	-6,62
2n	-7,55	-8,44	-7,36	-7,80	-4,40	-6,64	-8,07	-6,93	-3,80	-3,09	-7,22
3a	-10,95	-8,90	-12,82	-12,81	-12,31	-21,71	-15,17	-12,93	-11,41	-12,14	-9,06
3b	-9,39	-8,87	-13,10	-13,20	-12,18	-21,17	-14,73	-12,97	-10,61	-12,39	-7,85
3c	-8,90	-9,08	-13,07	-13,08	-11,66	-20,79	-14,75	-13,19	-8,59	-12,57	-6,04
3d	-11,41	-8,62	-12,15	-13,97	-12,02	-22,42	-15,40	-12,80	-11,12	-12,39	-9,68
3e	-9,08	-9,52	-13,85	-12,61	-12,25	-20,21	-14,26	-12,13	-9,99	-11,39	-7,12
3f	-8,75	-9,39	-12,48	-12,83	-11,37	-21,10	-14,44	-12,48	-9,20	-11,80	-6,37
3g	-8,14	-8,24	-12,27	-11,89	-11,40	-19,69	-13,89	-11,50	-9,57	-11,01	-6,75
3h	-8,62	-8,63	-12,40	-12,74	-11,06	-20,02	-14,59	-12,16	-9,33	-11,98	-6,80
3i	-9,59	-10,47	-13,33	-13,21	-12,67	-20,34	-15,79	-13,34	-10,05	-13,49	-7,43
3j	-12,08	-9,02	-12,23	-13,59	-11,82	-21,51	-15,25	-12,59	-10,00	-12,19	-9,14
3k	-9,06	-9,04	-12,29	-12,44	-11,36	-19,75	-14,67	-12,27	-9,30	-11,92	-5,85
3l	-9,62	-9,91	-13,15	-13,05	-12,24	-20,86	-15,40	-13,46	-9,66	-12,90	-6,60
3m	-8.76	-10.44	-13.24	-12.50	-11.79	-20.13	-15.17	-12.74	-9.47	-12.25	-7.27
4a	-6.93	-9.90	-7.70	-7.17	-8.26	-6.89	-7.84	-6.98	-7.54	-6.72	-8.23
4b	-7,01	-10,07	-7,85	-7,57	-8,23	-7,07	-8,18	-7,28	-7,22	-6,90	-8,33
4c	-6,86	-10,15	-8,10	-7,63	-8,13	-7,48	-8,53	-7,44	-6,15	-8,01	-8,41

As can be seen, the vast majority of the RMSD scores are around the expected value, since there are always divergences associated with the elimination in the molecular coupling calculation of water molecules and ions used during the crystallization process, Another factor to take into account is the size of the ligand, which seems to be

the cause of the value of 5,76 in the case of posaconazole, which has a molar weight of 700,78 g·mol^{-1}.[25]

All pseudopeptic imidazoles in schemes 1 and 3 show lower normalized docking scores than their respective co-crystallized ligands and, except for CYP51-*L.infantum*, also show lower normalized docking scores than fluconazole. It is also remarkable that for CYP51-*C.glabrata* schemes 1 and 3 show the lowest values of normalized docking scores in the entire study. It can be seen that these compounds form coordinated bonds with the Fe^{2+} cation of the heme group through the carbonyl group of the aspartic acid substituent, while the other carbonyl group is free to form a hydrogen bond with amino acid residues of the active site (Figure 2), while establishing a significant number of hydrophobic interactions.

A B

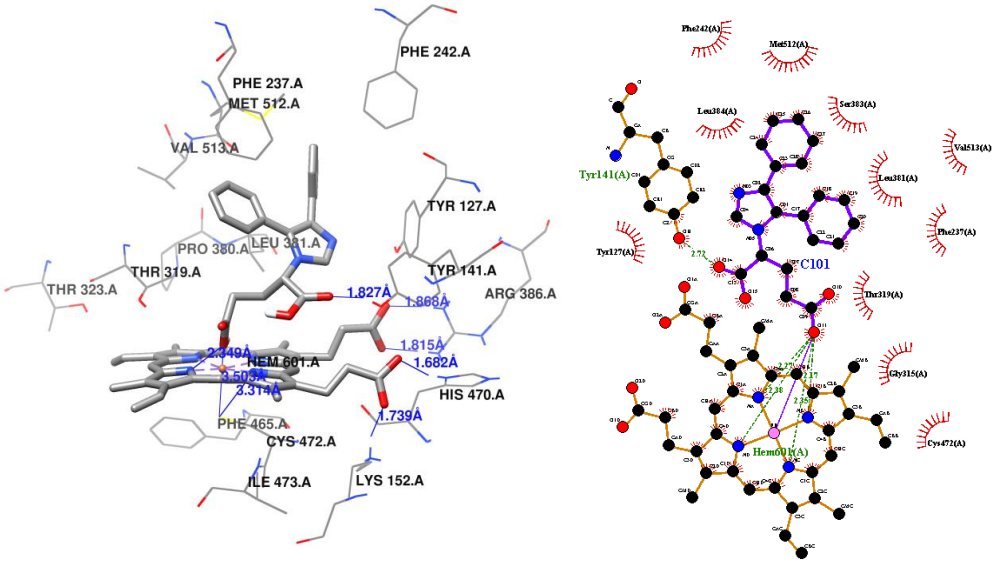

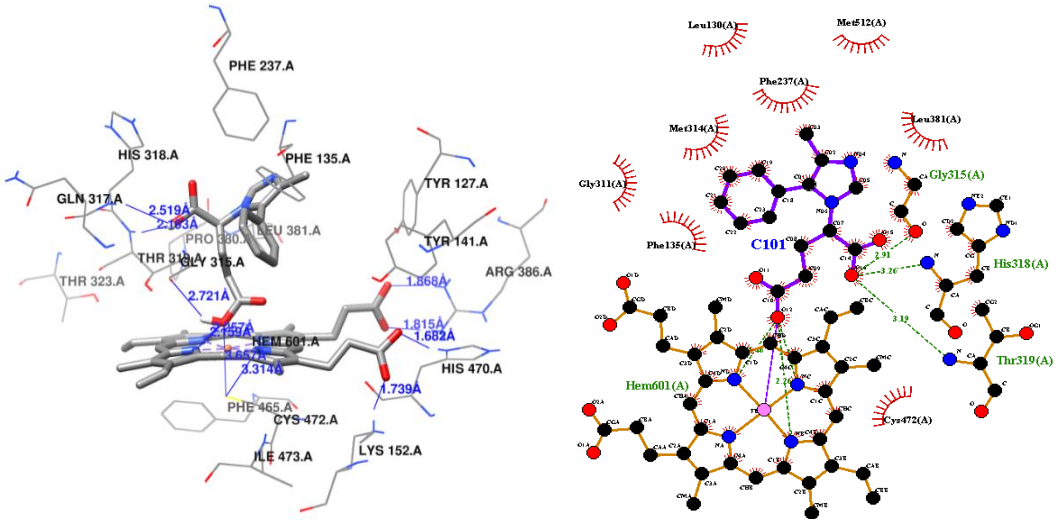

C D

Fig. 2- Lowest-energy docked poses with the CYP51-*C.glabrata* (PDB: 5JLC). (**A, B**) **1d** compound (**C, D**) **3d** compound

A B

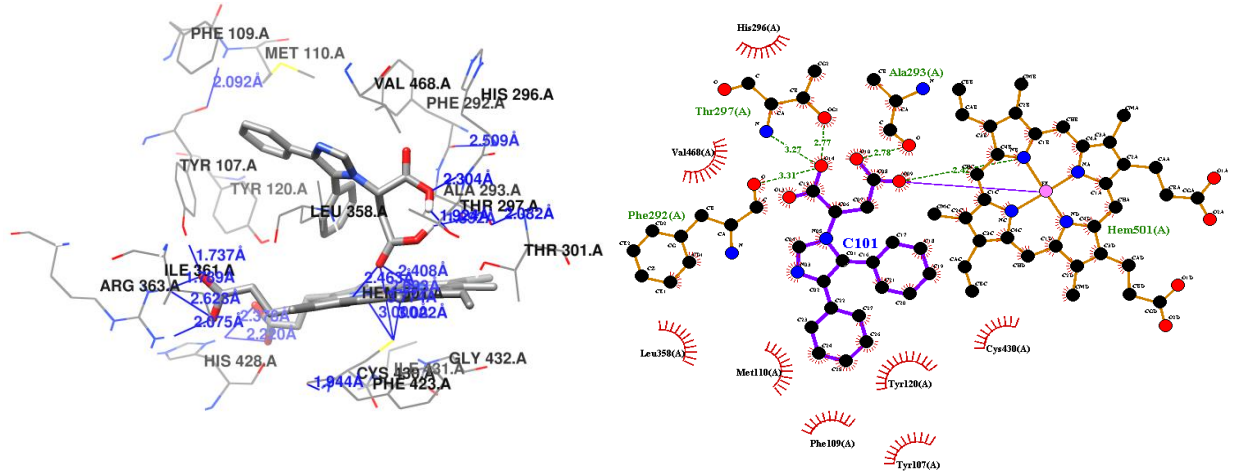

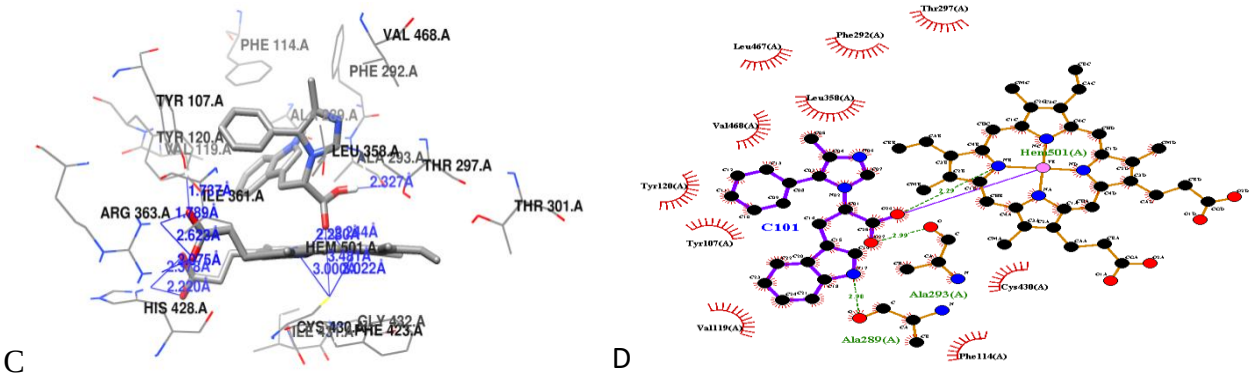

Fig. 3- Lowest-energy docked poses with the CYP51-*N.fowleri* (PDB: 5TL8). (**A, B**) **1k** compound (**C, D**) **3i** compound

In the case of CYP51-*N.fowleri*, the values of normalized docking scores are not comparable to those obtained against CYP51-*C.glabrata*, but they can also be considered excellent for schemes 1 and 3. As can be seen (Figure 3), the geometric arrangement of compounds **1k** and **3i** is very similar to each other and very similar to the behavior of CYP51-*C.glabrata.*

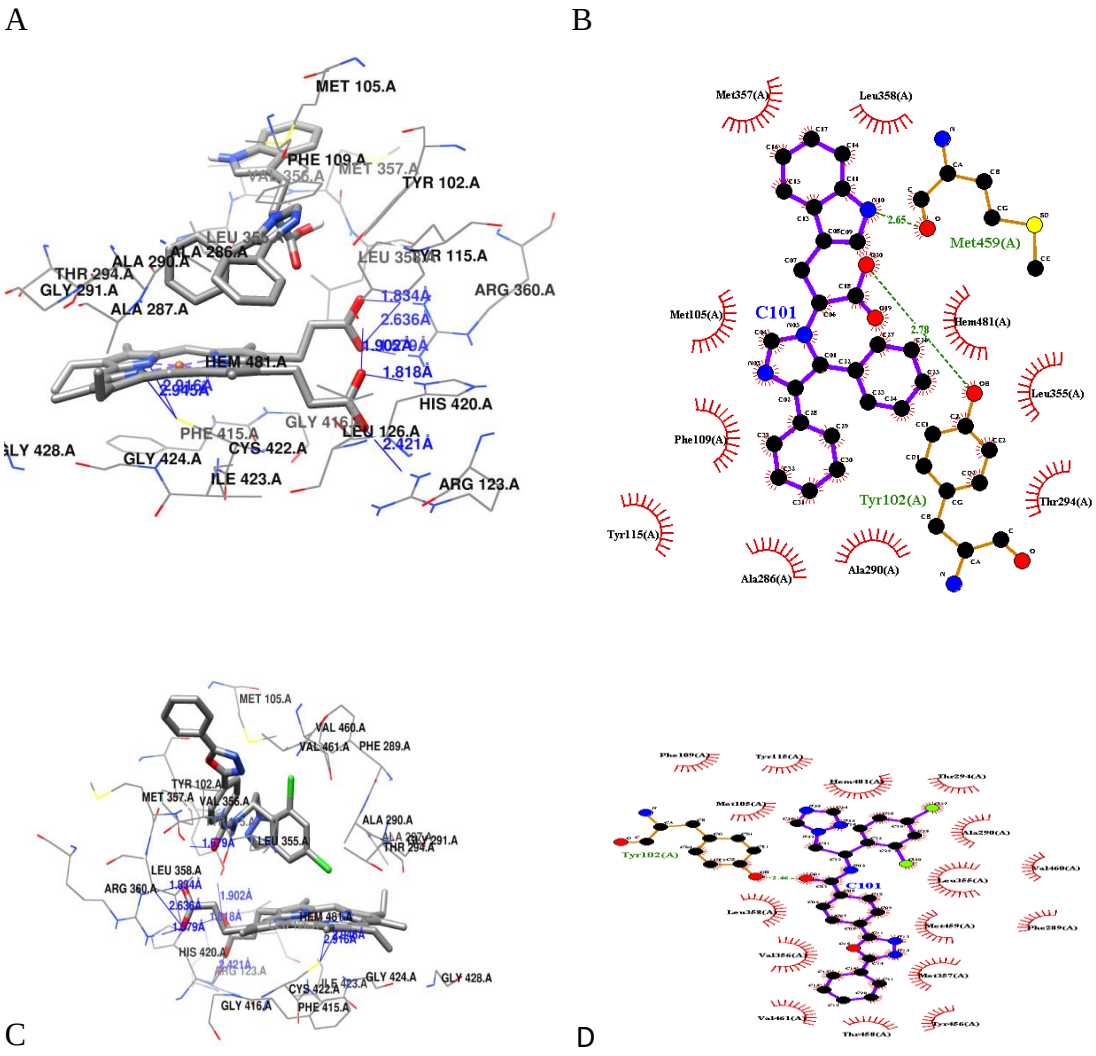

Fig. 4- Lowest-energy docked poses with the CYP51-*L.infantum* (PDB: 3L4D). (**A, B**) **1j** compound (**C, D**) fluconazole

It seems to be the conformation that provides stability to the protein-ligand complexes, in the case of these pseudopeptidic imizaloles with amino acid residues in position 1, it is when the carbonyl group has the possibility of interacting with the Fe^{2+} cation of the heme group. This is the case in all the proteins studied except in CYP51-*L.infantum.* The nature of the active site may be the reason for this behavior, which is very rigid and small, therefore, unlike fluconazole, pseudopeptidic imizaloles cannot directly interact with the Fe^{2+} cation of the heme group (Figure 4), which limits the stability of these

compounds. However, compounds such as **1j** present comparable results to fluconazole, given the large number of hydrophobic interactions with the amino acid residues in the cavity.

The behavior of Schemes 2 and 4 is different from Schemes 1 and 3. The compounds of Scheme 2 adopt a conformation similar to closed scissors, where the phenyl substituents at positions 4 and 5 parallel the “scissors” and the amino acid fragment with the “blades” (Figure 5). Interestingly, the “scissors” come close to the heme group, and not the "blades". This makes it impossible for the formation of hydrogen bonds and coordinated bonds between the ligands and the heme group, which is why these complexes formed they are not as stable as those in schemes 1 and 3, in addition to being poorly specific and probably continually form and break under the effect of concentration. Not surprisingly, the normalized docking scores are generally lower than those obtained for fluconazole.

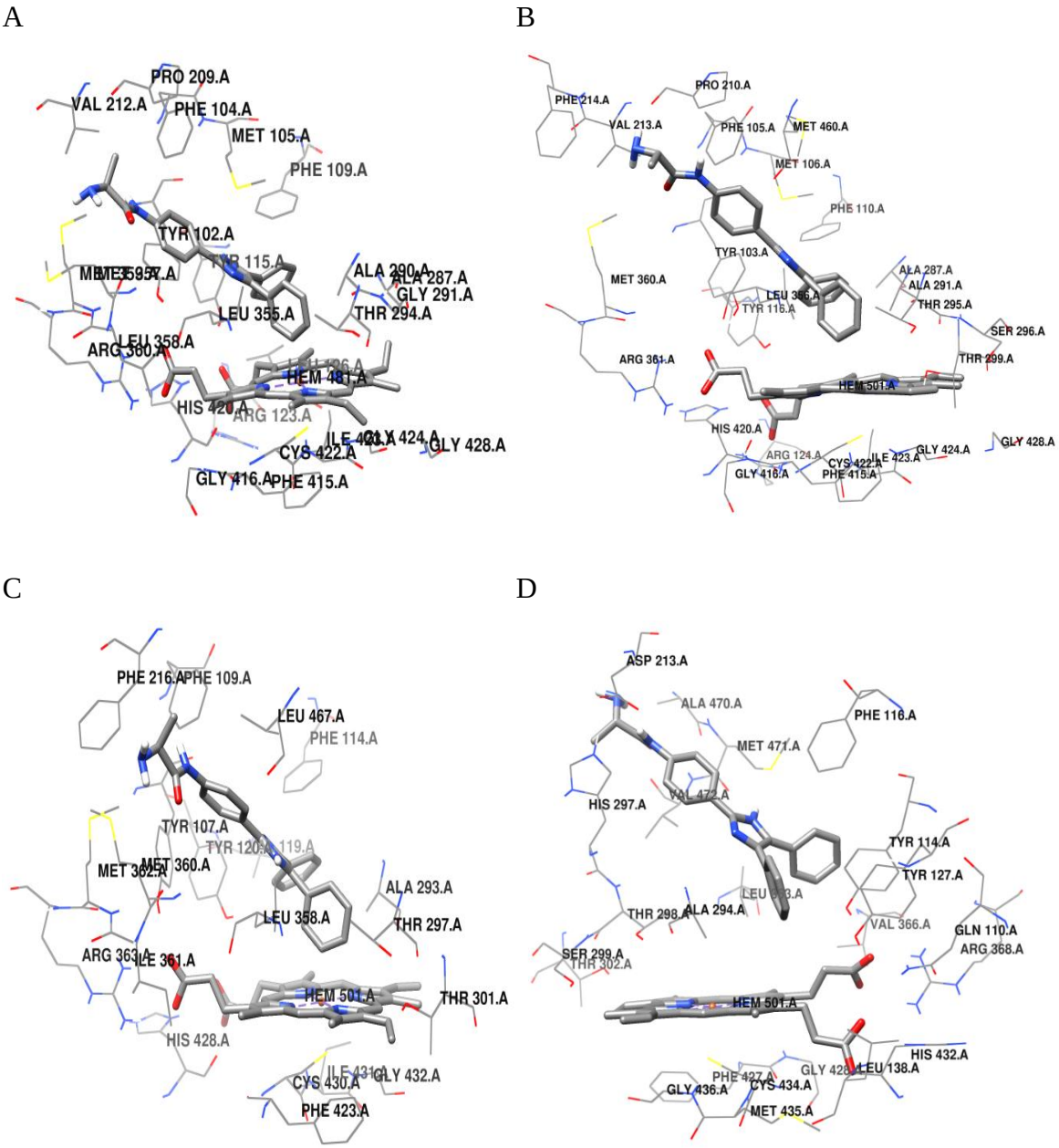

Fig. 5- 2b compound lowest-energy docked poses with the (**A**) CYP51-*L.infantum* (PDB: 3L4D) (**B**) CYP51-*T.brucei* (PDB: 4G3J) (**C**) CYP51- *N.fowleri* (PDB: 5TL8) (**D**) CYP51-*A.castellanii* (PDB: 6Q2C)

For the compounds of scheme 4 the parallelism with the shears is not valid (Figure 6), but in essence, the behavior is similar. In most cases, it is the phenyl group at the 4 position that is close to the heme group. This makes it impossible to form hydrogen

bonds and coordinate bonds with it. Even when the amino acid fragment enters the cavity, it cannot access the Fe^{2+} cation due to the low flexibility of these compounds with an important conjugation effect. As in scheme 2, the normalized docking score values are generally lower than fluconazole.

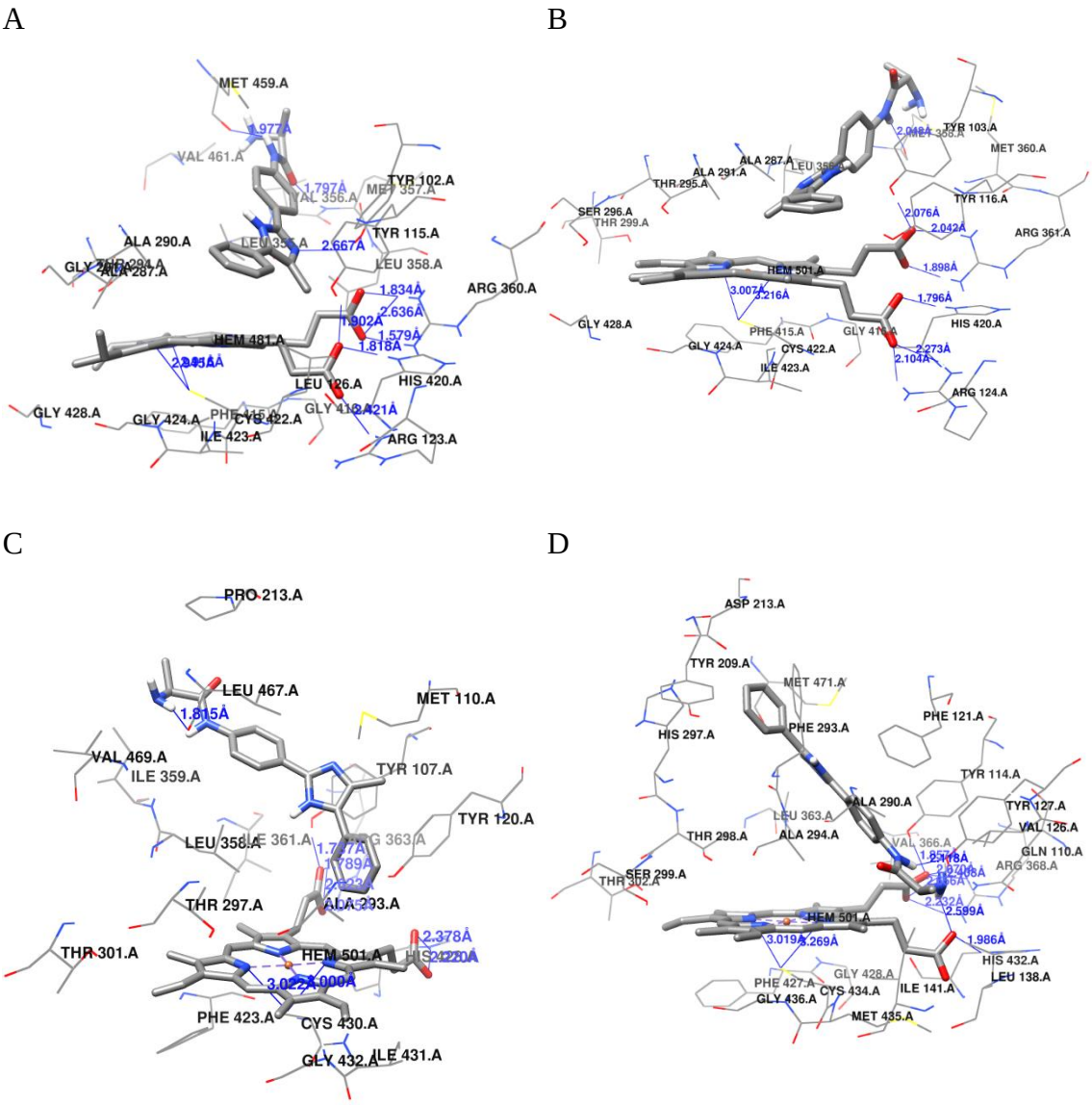

Fig. 6- 4b compound lowest-energy docked poses with the (**A**) CYP51-*L.infantum* (PDB: 3L4D) (**B**) CYP51-*T.brucei* (PDB: 4G3J) (**C**) CYP51- *N.fowleri* (PDB: 5TL8) (**D**) CYP51-*A.castellanii* (PDB: 6Q2C)

The precursor imidazoles behave in such a way that the lowest normalized docking score values correspond, in general, to the compounds that are substituted with nitrophenyl in position 2 (**p0**5, **p06**, **p11**, **p12**, **p17**, **p18**, **p23**, **p24**, **p29**, **p30**, **p35** and **p36**). This is because these compounds can establish interactions with the Fe^{2+} cation of the heme group (Figure 7). Compounds with m-nitrophenyl substituent in position 2 present lower normalized docking score values than compounds with p-nitrophenyl substituent in position 2, which seem to be more prevented from approaching the Fe^{2+} cation. It changes depending on the protein, but what is common is that when the nitro group manages to interact with the heme group, the normalized docking score decreases by around 1.5 kcal.

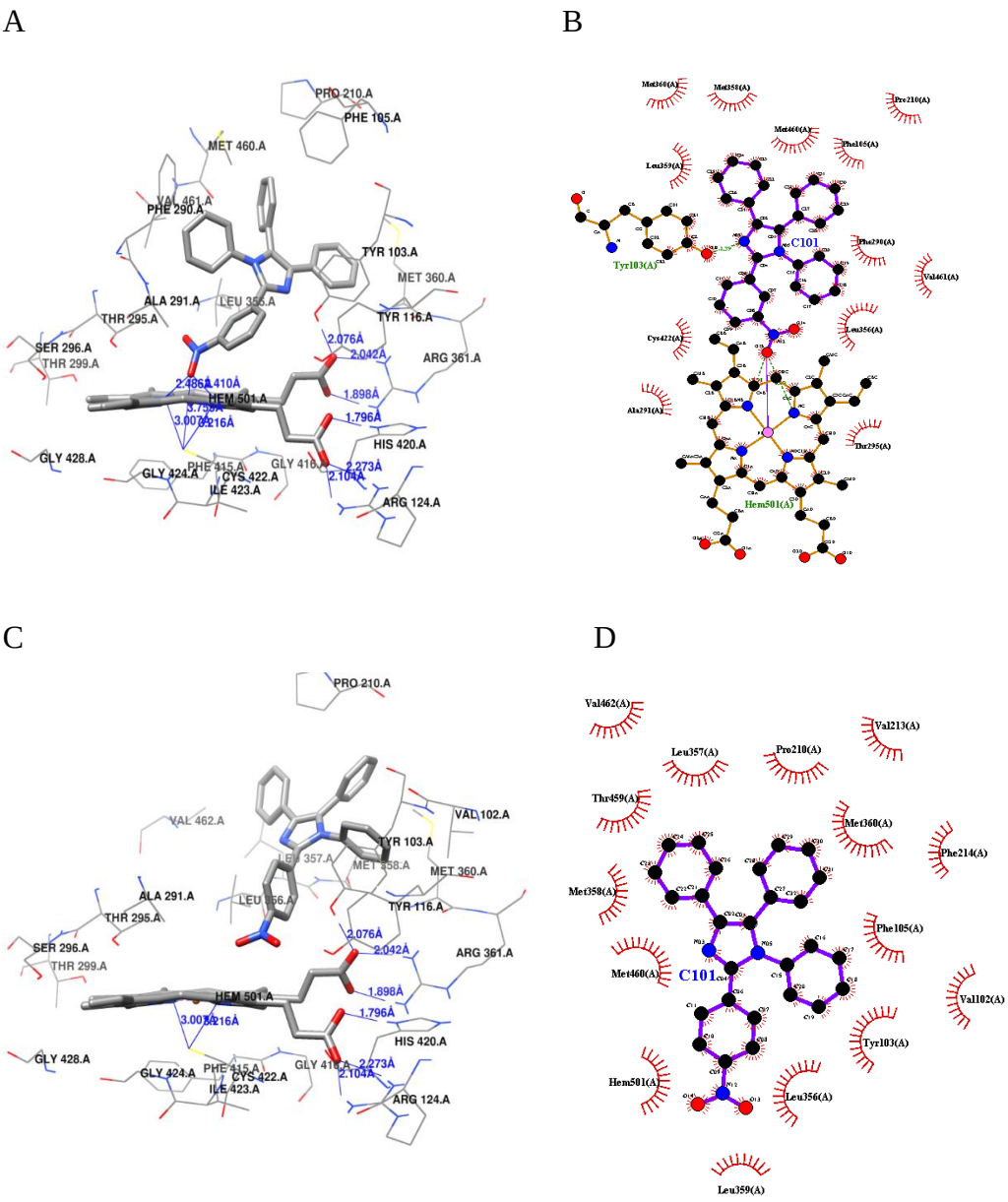

Fig. 7-Lowest-energy docked poses with the CYP51-*T.brucei* (PDB: 4G3J). (**A, B**) **p05** compound (**C, D**) **p06** compound.

However, before analyzing the possibilities of these compounds as inhibitors of one or another pathogen based on the selectivity coefficient with respect to CYP51-*H.sapiens* (Table 4).

Table 4. Estimated selectivity coefficient of pseudopeptic imidazoles with CYP51 molecular targets with respect to CYP51-*H.sapiens.*

Comp.	1x8v	314d	4c27	4g3j	4uym	5jlc	5tl8	5tz1	6q2c	7tef
1a	0,0	0,0	2,4	1,2	0,1	>2000	339,2	7,1	0,7	>2000
1b	0,0	0,0	0,9	0,7	0,1	>2000	35,1	7,9	0,2	>2000
1c	0,0	0,0	0,7	0,0	0,1	>2000	3,5	4,3	0,0	>2000
1d	0,1	0,0	2,2	3,2	0,6	>2000	211,8	18,0	0,1	1600,1
1e	0,0	0,1	1,0	0,3	0,1	>2000	0,6	2,0	0,0	1999,4
1f	0,0	0,0	0,5	1,0	0,2	>2000	9,5	10,5	0,0	>2000
1g	0,0	0,0	1,5	0,2	0,1	>2000	0,9	8,8	0,0	>2000
1h	1	0,0	1,5	0,2	0,2	>2000	132,2	4,9	0,0	>2000
1i	0,0	0,0	1,6	1,6	0,1	>2000	44,4	10,6	0,0	>2000
1j	0,0	0,0	0,4	0,1	0,0	>2000	0,7	2,4	0,0	>2000
1k	0,4	0,0	2,0	1,2	0,3	>2000	286,2	8,6	0,1	>2000
1l	0,4	0,0	2,9	1,5	0,3	>2000	292,7	9,8	0,1	>2000
1m	0,3	0,0	2,3	1,2	0,2	>2000	258,2	8,0	0,1	>2000
1n	0,4	0,0	2,7	1,4	0,3	>2000	358,4	10,0	0,1	>2000
2a	201,3	>2000	351,4	656,2	10,9	80,9	951,2	751,0	138,8	0,0
2b	291,3	>2000	815,5	1068,4	27,0	553,1	677,3	1864,7	2,9	0,0
2c	>2000	>2000	>2000	>2000	47,3	>2000	>2000	>2000	7,2	0,0
2d	>2000	>2000	>2000	>2000	2,1	137,4	>2000	596,6	0,0	0,0
2e	>2000	>2000	1013,6	>2000	7,0	254,0	>2000	516,0	2,1	0,0
2f	>2000	>2000	>2000	>2000	11,2	73,9	>2000	1119,0	2,1	0,0
2g	>2000	>2000	>2000	>2000	13,1	>2000	>2000	>2000	1,8	0,0
2h	>2000	>2000	1 747,6	>2000	14,5	764,3	>2000	845,8	6,4	0,0
2i	216,5	>2000	>2000	>2000	0,3	278,9	>2000	>2000	0,0	0,0
2j	>2000	>2000	888,5	>2000	4,0	11,8	>2000	509,0	0,1	0,0
2k	>2000	>2000	>2000	>2000	0,9	60,8	>2000	>2000	0,0	0,0
2l	>2000	>2000	>2000	>2000	30,9	845,6	>2000	>2000	0,4	0,0
2m	3,2	230,8	11,4	27,1	9,8	2,5	94,3	11,8	0,4	0,4
2n	1 845,7	>2000	1 339,4	>2000	9,1	397,3	>2000	648,2	3,3	0,0
3a	0,1	0,0	3,2	3,1	1,3	>2000	167,7	3,8	0,3	181,9
3b	0,0	0,0	3,3	3,9	0,7	>2000	51,7	2,6	0,0	>2000
3c	0,0	0,0	2,3	2,4	0,2	>2000	39,8	2,9	0,0	>2000
3d	0,2	0,0	0,7	14,4	0,5	>2000	160,3	2,0	0,1	97,6
3e	0,0	0,0	62,9	7,8	4,2	>2000	126,2	3,5	0,1	1 356,6
3f	0,0	0,0	3,2	5,8	0,5	>2000	86,2	3,2	0,0	>2000
3g	0,0	0,0	8,5	4,4	1,9	>2000	129,2	2,3	0,1	1 315,6
3h	0,0	0,0	2,0	3,6	0,2	>2000	81,5	1,3	0,0	>2000
3i	0,0	0,0	0,8	0,6	0,3	>2000	48,4	0,8	0,0	>2000
3j	0,8	0,0	1,1	10,6	0,5	>2000	174,6	2,0	0,0	171,3
3k	0,0	0,0	1,9	2,4	0,4	>2000	102,5	1,8	0,0	>2000
3l	0,0	0,0	1,5	1,3	0,3	>2000	67,9	2,6	0,0	>2000
3m	0,0	0,0	5,3	1,5	0,5	>2000	138,0	2,3	0,0	>2000
4a	1,4	215,3	5,3	2,1	13,4	1,3	6,6	1,6	4,0	0,1
4b	1,2	209,7	4,9	3,1	9,4	1,3	8,6	1,9	1,7	0,1
4c	0,1	36,9	1,2	0,5	1,2	0,4	2,4	0,4	0,0	0,5

Since the highest selectivity is usually related to, a lower weight in the interaction with the Fe^{2+} cation of the heme group of these proteins. That is, the interactions with the amino acid residues that make up the active site are of greater importance. Figure 8

analyzes the lowest-energy docked poses of **1j**, **2j**, **3j**, **4j**, **p1** and **p23** with the CYP51-*H.sapiens*, as representative compounds of their respective schemes.

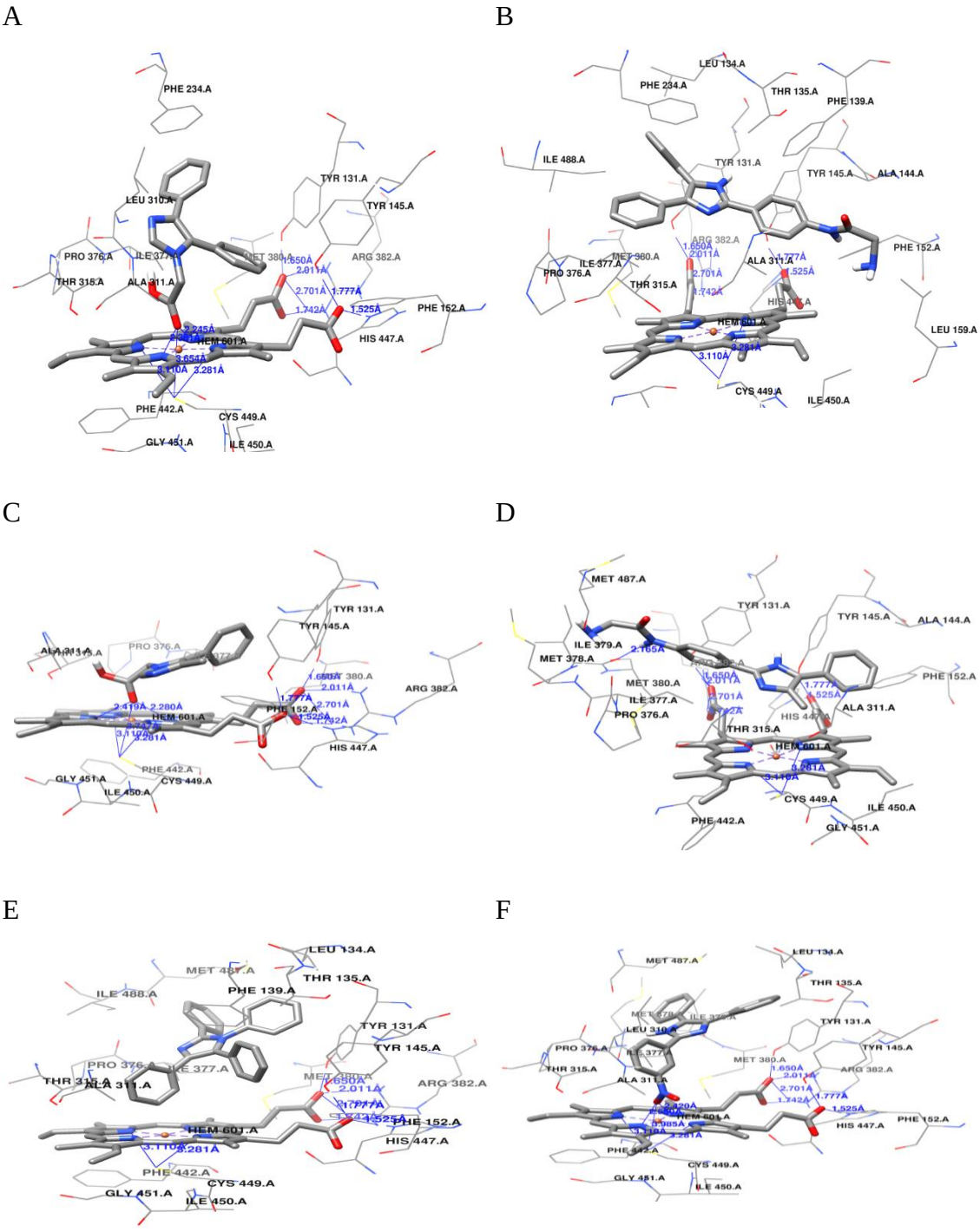

Fig. 8-Lowest-energy docked poses with the CYP51-*H.sapiens* (PDB: 6UEZ). (**A**) **1j** compound (**B**) **2j** compound (**C**) **3j** compound (**D**) **4j** compound (**E**) **p1** compound (**F**) **p23** compound

The geometry of the protein-ligand complexes **2j** and **4j** show that there are no interactions with the Fe^{2+} cation of the heme group, which explains their low selectivity, as well as their high binding free energy values compared to the other schemes. The complex with ligand **3j** should behave in a similar way to **2j**, but the change of the phenyl group to the methyl group allows the ligand to be oriented in a very different way. Although there is no direct interaction with the Fe^{2+} cation of the heme group, this ligand scheme is located in a similar way in all proteins, being very non-selective.

In the case of schemes 1 and 3, it can be seen that there is a direct interaction with the Fe^{2+} cation of the heme group, so the difference between the phenyl and methyl substituent hardly influences the selectivity. In fact, the conformations that these ligands adopt, which are relatively small, are very similar.

The precursor ligands behave differently depending on polar groups existing or not. Those that have polar groups, such as the **p23** compound, interact with the Fe^{2+} cation of the heme group through strong bonds that make them very unselective. However, those that do not have polar groups are also unselective, which is because these highly conjugates structures can interact with the heme group through the π electron clouds. This, along with the hydrophobic interactions with the rest of the active site, do not provide much stability for any of the proteins, so the selectivity of these compounds is rather variable.

Conclusions

The pseudopeptic imidazoles studied show, in general, acceptable values of normalized docking scores against pathogenic proteins. The high selectivity of scheme 2 against pathogenic proteins is shown, in contrast to scheme 1, except for CYP51-*C.glabrata*. Considering both parameters, it can be said that: although it seems that none of the compounds achieves effective results against CYP51-*M.marinum* and CYP51-*A.fumigatus*, it is achieved against the rest of the proteins. The interaction of scheme 1 against CYP51-*C.glabrata* stands out due to its high selectivity and its low normalized docking scores. It can be seen that the interaction of both schemes is different. The compounds in scheme 1 coordinate directly with the Fe^{2+} ion of the heme group, while the compounds in scheme 2 interact through the π orbitals of the benzene rings.

Acknowledgment

This research was carried out in the Supercomputer of the Universidad de Oriente, which is part of the Cuban Supercomputing Center (HPC-Cuba) with the support of the VLIR-UOS JOINT project and the Ibero-American Supercomputing Network (RICAP)

References

1. LEPESHEVA, G. I. AND M. R. WATERMAN "CYP51—the omnipotent P450". *Molecular and cellular endocrinology*, 2004, **215**(1-2), 165-170. https://doi.org/10.1016/j.mce.2003.11.016.

2. LEPESHEVA, G. I., T. Y. HARGROVE, Y. KLESHCHENKO, W. D. NES, *et al*. "CYP51: A major drug target in the cytochrome P450 superfamily". *Lipids*, 2008, **43**(12), 1117-1125. https://doi.org/10.1007/s11745-008-3225-y.

3. CHOI, J. Y., L. M. PODUST AND W. R. ROUSH "Drug strategies targeting CYP51 in neglected tropical diseases". *Chemical Reviews*, 2014, **114**(22), 11242-11271. https://doi.org/10.1021/cr5003134.

4. HARGROVE, T. Y., K. KIM, M. D. N. C. SOEIRO, C. F. DA SILVA, *et al*. "CYP51 structures and structure-based development of novel, pathogen-specific inhibitory scaffolds". *International Journal for Parasitology: Drugs and Drug Resistance*, 2012, **2**, 178-186. https://doi.org/10.1016/j.ijpddr.2012.06.001.

5. WARRILOW, A. G., C. L. PRICE, J. E. PARKER, N. J. ROLLEY, *et al*. "Azole antifungal sensitivity of sterol 14α-demethylase (CYP51) and CYP5218 from Malassezia globosa". *Scientific reports*, 2016, **6**(1), 1-10. https://doi.org/10.1038/srep27690.

6. ZHANG, J., L. LI, Q. LV, L. YAN, *et al.* "The fungal CYP51s: Their functions, structures, related drug resistance, and inhibitors". *Frontiers in microbiology*, 2019, **10**, 691. https://doi.org/10.3389/fmicb.2019.00691.

7. ZHANG, H.-Z., L.-L. GAN, H. WANG AND C.-H. ZHOU "New progress in azole compounds as antimicrobial agents". *Mini reviews in medicinal chemistry*, 2017, **17**(2), 122-166. https://doi.org/10.2174/1389557516666160630120725.

8. WARRILOW, A. G., J. E. PARKER, C. L. PRICE, E. P. GARVEY, et al. "The tetrazole VT-1161 is a potent inhibitor of Trichophyton rubrum through its inhibition of T. rubrum CYP51". *Antimicrobial agents and chemotherapy*, 2017, **61**(7), e00333-00317. https://doi.org/10.1128/aac.00333-17.

9. VERMA, A. K., A. MAJID, M. HOSSAIN, S. AHMED, et al. "Identification of 1, 2, 4-triazine and its derivatives against Lanosterol 14-demethylase (CYP51) property of Candida albicans: Influence on the development of new antifungal therapeutic strategies". *Frontiers in medical technology*, 2022, 16. https://doi.org/10.3389/fmedt.2022.845322.

10. DOYLE, P. S., C.-K. CHEN, J. B. JOHNSTON, S. D. HOPKINS, et al. "A nonazole CYP51 inhibitor cures Chagas' disease in a mouse model of acute infection". *Antimicrobial agents and chemotherapy*, 2010, **54**(6), 2480-2488. https://doi.org/10.1128/aac.00281-10.

11. HASSAN, E. A., I. A. SHEHADI, A. M. ELMAGHRABY, H. M. MOSTAFA, et al. "Synthesis, molecular docking analysis and in vitro biological evaluation of some new heterocyclic scaffolds-based indole moiety as possible antimicrobial agents". *Frontiers in molecular biosciences*, 2022, 1238. https://doi.org/10.3389/fmolb.2021.775013.

12. COTUÁ, J., H. LLINÁS AND S. COTES "Virtual Screening Based on QSAR and Molecular Docking of Possible Inhibitors Targeting Chagas CYP51". *Journal of Chemistry*, 2021, **2021**. https://doi.org/10.1155/2021/6640624.

13. WARRILOW, A. G., J. E. PARKER, D. E. KELLY AND S. L. KELLY "Azole affinity of sterol 14α-demethylase (CYP51) enzymes from Candida albicans and Homo sapiens". *Antimicrobial agents and chemotherapy*, 2013, **57**(3), 1352-1360. https://doi.org/10.1128/aac.02067-12.

14. IRANNEJAD, H., S. EMAMI, H. MIRZAEI AND S. M. HASHEMI "In silico prediction of ATTAF-1 and ATTAF-2 selectivity towards human/fungal lanosterol 14α-demethylase using molecular dynamic simulation and docking approaches". *Informatics in Medicine Unlocked*, 2020, **20**, 100366. https://doi.org/10.1016/j.imu.2020.100366.

15. BERMAN, H. M., T. BATTISTUZ, T. N. BHAT, W. F. BLUHM, et al. "The protein data bank". *Acta Crystallographica Section D: Biological Crystallography*, 2002, **58**(6), 899-907. https://doi.org/10.1107/S0907444902003451.

16. O'BOYLE, N. M., M. BANCK, C. A. JAMES, C. MORLEY, et al. "Open Babel: An open chemical toolbox". *Journal of cheminformatics*, 2011, **3**(1), 1-14. https://doi.org/10.1186/1758-2946-3-33.

17. PETTERSEN, E. F., T. D. GODDARD, C. C. HUANG, G. S. COUCH, et al. "UCSF Chimera—a visualization system for exploratory research and analysis". *Journal of computational chemistry*, 2004, **25**(13), 1605-1612. https://doi.org/10.1002/jcc.20084.

18. SOLIS-VASQUEZ, L., A. F. TILLACK, D. SANTOS-MARTINS, A. KOCH, et al. "Benchmarking the performance of irregular computations in AutoDock-GPU molecular docking". *Parallel Computing*, 2022, **109**, 102861. https://doi.org/10.1016/j.parco.2021.102861.

19. LASKOWSKI, R. A. AND M. B. SWINDELLS. LigPlot+: multiple ligand–protein interaction diagrams for drug discovery. In.: ACS Publications, 2011. https://doi.org/10.1021/ci200227u.

20. DA SILVA, J. K. R., P. L. B. FIGUEIREDO, K. G. BYLER AND W. N. SETZER "Essential oils as antiviral agents, potential of essential oils to treat SARS-CoV-2 infection: An in-silico investigation". *International journal of molecular sciences*, 2020, **21**(10), 3426. https://doi.org/10.3390/ijms21103426.

21. BELL, E. W. AND Y. ZHANG "DockRMSD: an open-source tool for atom mapping and RMSD calculation of symmetric molecules through graph isomorphism". *Journal of cheminformatics*, 2019, **11**(1), 1-9. https://doi.org/10.1186/s13321-019-0362-7.

22. ARBA, M., S. IHSAN AND D. H. TJAHJONO "In silico study of porphyrin-anthraquinone hybrids as CDK2 inhibitor". *Computational Biology and Chemistry*, 2017, **67**, 9-14. https://doi.org/10.1016/j.compbiolchem.2016.12.005.

23. VARGAS, J. A. R., A. G. LOPEZ, M. C. PIÑOL AND M. FROEYEN "Molecular docking study on the interaction between 2-substituted-4, 5-difuryl Imidazoles with different Protein Target for antileishmanial activity". *Journal of Applied*

Pharmaceutical Science, 2018, **8**(3), 014-022. http://dx.doi.org/10.7324/JAPS.2018.8303.

24. HEVENER, K. E., W. ZHAO, D. M. BALL, K. BABAOGLU, et al. "Validation of Molecular Docking Programs for Virtual Screening against Dihydropteroate Synthase". *J Chem Inf Model*, 2009, **49**(2), 444-460. https://doi.org/10.1021/ci800293n.

25. ZINAD, D. S., A. MAHAL, S. SISWODIHARDJO, M. R. F. PRATAMA, et al. "3D-Molecular Modeling, Antibacterial Activity and Molecular Docking Studies of Some Imidazole Derivatives". *Egyptian Journal of Chemistry*, 2021, **64**(1), 93-105. https://dx.doi.org/10.21608/ejchem.2020.31043.2662.

Conflicts of interest

The authors express that there are no conflicts of interest in the submitted manuscript.

Author contributions

Yonatan Mederos-Nuñez: active participation in the discussion of the results: Review and approval of the final version of the work.

Raidel Rosales Rosabal, Rebeca Joa Acree: active participation in the discussion of the results

Armando Ferrer Serrano, América García-López: review and approval of the final version of the work.

All author shave read and agreed to the published version ofthe manuscript.